



Massive Quark Self-Energy in Cavity QCD

J A Cuthbert
Department of Physics
University of Cape Town

A thesis submitted in partial fulfillment
of the requirements for
the degree of Master of Science
in
Theoretical Physics

September 17, 1991

The copyright of this thesis vests in the author. No quotation from it or information derived from it is to be published without full acknowledgement of the source. The thesis is to be used for private study or non-commercial research purposes only.

Published by the University of Cape Town (UCT) in terms of the non-exclusive license granted to UCT by the author.

Abstract

The greatest obstacle in calculating the self-energy Feynman diagram is that it is, in principle, linearly divergent. So far the self-energy of a massive quark in cavity quantum chromodynamics has only been calculated for the lowest cavity mode $1s_{1/2}$. The methods used so far, have been based on the multiple reflection formalism, in which the zero reflection term is extracted out analytically and evaluated separately using Pauli-Villars regularization.

This thesis is based on the dimensional regularization scheme, adapted for use in the cavity, by Stoddart *et al.*, who calculated the self-energy for a massless quark. This involves analytically isolating the divergences using dimensional regularization and then removing the divergences using the minimal subtraction (ms) scheme or some similar subtraction scheme. In this thesis, the self-energies of massive quarks have been calculated using the ms scheme for a number of low-lying cavity modes. The $1s_{1/2}$ results have also been compared with the Pauli-Villars regularization scheme used by Goldhaber, Jaffe and Hansson.

Contents

1	Introduction	4
1.1	Dimensional Regularization in the Cavity	5
1.2	Units	6
2	Fourier Transforms and propagators	8
2.1	Quark Propagator	8
2.2	Gluon Propagator	10
2.3	Fourier transform of $(\not{s} - 4m)$	10
3	Calculation of Quark Self-Energy in Free Space	12
3.1	The Feynman Diagram	12
3.2	Regularization	13
3.3	Renormalization	16
3.3.1	Minimal Subtraction Scheme	16
3.3.2	Mass Renormalization Scheme	16
4	Calculation of Quark Self-Energy in a cavity	19
4.1	Calculation of Σ^C	19
4.2	Minimal Subtraction Scheme	21
4.3	Energy Conservation	22
4.4	Mass Renormalization Scheme	26
4.5	Accuracy of Results	28

5	Conclusion	30
5.1	Acknowledgements	30
A	Mathematical appendices	31
A.1	Gamma Matrix Identities in D Dimensions	31
A.2	Conversion to Euclidean Space	32
A.3	Some Common Integrals	32
A.4	The Gamma Function	33
B	Cavity modes	35
B.1	Quarks	35
B.2	Gluons	36
C	The Vertex Integrals	39
C.1	The qqg Vertex	39
C.2	The qqg Sum Rule	40
	Bibliography	42

Chapter 1

Introduction

The quark self-energy is of considerable interest to us since it makes an important contribution to the hadronic mass spectrum. The quark self-energy, however, is superficially linearly divergent, which makes it difficult to calculate.

Only a few people have evaluated the quark self-energy in a cavity up until now. Baacke *et al.* [1] have calculated the massive quark self-energy for the $1s_{1/2}$ state in the Coulomb gauge. Their calculation uses an analytical separation of direct and reflected terms. Later Goldhaber, Hansson and Jaffe used the propagators, written in a Multiple Reflection Expansion (MRE) [2, 3], to calculate the $1s_{1/2}$ massive quark self-energy in the Feynman gauge [4, 5, 6]. Finally Stoddart and Viollier [7, 8] (hereafter referred to as [SV]) developed a technique, using the method of dimensional regularization, to calculate the massless quark self-energy, in a cavity, for a number of low lying states, including the $1s_{1/2}$ state.

In this thesis, the self-energy of a massive quark is calculated in the Feynman gauge, to order α_s , for a number of low lying cavity modes. The technique and notation developed in [SV] is used extensively. All our results are quoted in the \overline{ms} renormalization scheme.

In this chapter, a general outline of the technique used, as well as a brief discussion on units, is given. In Chapter 2, the necessary Fourier transforms and propagators required for use in the cavity are obtained. In chapter 3, the quark self-energy in free space is calculated, in order to obtain the free space subtraction factor. The technique of dimensional regularization used here is outlined in detail. In chapter 4, the quark self-energy in a cavity is calculated. All the numerical results are in this chapter. In chapter 5, conclusions are drawn. In appendix A, some mathematical tools used for the

regularization are included. In appendix B, the cavity modes are detailed. In appendix C, the vertex integrals are listed.

1.1 Dimensional Regularization in the Cavity

The self-energy is in principle linearly divergent. Using dimensional regularization, the divergence is isolated unambiguously. This divergence is then removed using some renormalization scheme.

The first step of this procedure, is to represent the number of space time dimensions by D . The self-energy calculated in dimensions $D \neq 4$ yields a finite result. This leads one to proceed by generalizing the number of dimensions to $D = 4 - 2\epsilon$, where ϵ is a small finite variable, the intention being to return back to four space time dimensions at the end of the calculation, by applying the limit $\epsilon \rightarrow 0$. The divergence then manifests itself as a pole in the infinitesimal variable ϵ which can be separated out from the other terms. This is written as

$$\Sigma^0(\epsilon) = F + S(\epsilon). \quad (1.1)$$

$S(\epsilon)$ is the singular term which is in the form $(1/\epsilon + \text{constant})$. The *constant* is dependent on the particular renormalization scheme chosen.

F , which is also known as the ‘renormalized’ self-energy, sometimes written as Σ_R^0 , is the finite quantity of interest to us. F is evaluated in the following manner:

$$F = \lim_{\epsilon \rightarrow 0} [\Sigma^0(\epsilon) - S(\epsilon)]. \quad (1.2)$$

The explicit form of the divergence is proportional to the gamma function

$$\Gamma(\epsilon) = \int_0^\infty dz z^{-1+\epsilon} e^{-z}, \quad (1.3)$$

which is extremely convenient since it allows $S(\epsilon)$ to be written as

$$S(\epsilon) = \int_0^\infty dz S(\epsilon, z). \quad (1.4)$$

Here $S(\epsilon, z)$ is the integrand of the z integral. $S(\epsilon)$ is now in a form known as the z -form or the spectral form. So far the discussion has referred to the self-energy in free space. The cavity quark self-energy is simply related to the free space quark self-energy by the relation

$$\Sigma^C(\epsilon) = \Sigma^0(\epsilon) + \tilde{\Sigma}. \quad (1.5)$$

The term $\tilde{\Sigma}$ is the reflection piece due to the boundary and is finite in $D = 4$ dimensions, as has been shown by Hansson and Jaffe [2]. Using the analysis of the free space case, $\Sigma^C(\epsilon)$ is written as

$$\Sigma^C(\epsilon) = \Sigma^0(\epsilon) + \tilde{\Sigma} = S(\epsilon) + F + \tilde{\Sigma}. \quad (1.6)$$

Thus the z -form of $S(\epsilon)$ is calculated analytically by looking at the free space quark self-energy. Σ^C can also be written in the spectral form which allows the the finite part of interest, the renormalized cavity quark self-energy, to be extracted. Thus

$$\Sigma_R^C = F + \tilde{\Sigma} = \lim_{\epsilon \rightarrow 0} \int_0^\infty dz (\Sigma^C(\epsilon, z) - S(\epsilon, z)). \quad (1.7)$$

The order of the limit and the integral can be swapped so that the final form used to do the numerical calculation is

$$\Sigma_R^C = \int_0^\infty dz (\lim_{\epsilon \rightarrow 0} \Sigma^C(\epsilon, z) - \lim_{\epsilon \rightarrow 0} S(\epsilon, z)). \quad (1.8)$$

The integrand is ill-defined computationally for $z = 0$, where it exhibits a subtraction of two singularities. The whole integrand is replaced by an approximation for low z instead. The approximation is found by fitting a six or seven degree polynomial to the function $(\Sigma^C(0, z) - S(0, z))$ for some suitable z range, where $(\Sigma^C(0, z) - S(0, z))$ is still well behaved. This polynomial is then used in place of the original integrand for the z range near $z = 0$.

1.2 Units

Throughout this thesis, dimensionless units will be used. In this section, the dimensionless units are related to the familiar MeV fm units. The energy of the quark is given by

$$\epsilon = \epsilon_0 + \alpha_s \Sigma_n + O(\alpha_s^2) \quad (1.9)$$

in dimensionless units where Σ_n is the self-energy. In MeV units, the energy is related to ϵ by

$$E = \frac{\epsilon \hbar c}{R}, \quad (1.10)$$

where $\hbar c = 197.327\,053$ MeV fm and R is the radius of the cavity measured in fm. Thus the units of Σ_n throughout this thesis are quoted in units of $\alpha_s \hbar c / R$. Similarly the mass, M , is quoted in dimensionless units and is given by the relation

$$M = \frac{mc^2 R}{\hbar c}. \quad (1.11)$$

where mc^2 is in MeV. The invariant mass of light quarks as calculated in [9] and [10] are quoted in the table below together with the corresponding dimensionless units.

quark mass	MeV	Dimensionless Units
m_u	8.2 ± 1.5	0.042 ± 0.008
m_d	14.4 ± 1.5	0.073 ± 0.008
m_s	266 ± 29	1.35 ± 0.15

Chapter 2

Fourier Transforms and propagators

In this chapter the two cavity propagators which are used in chapter 4 are derived. By doing so, the notation used later on in this thesis is introduced. The Fourier transform of the quantity $(\not{p} - 4m)$ into cavity space is also obtained. The calculation will be done in momentum space since the propagators take on a simpler form in momentum space than in co-ordinate space.

2.1 Quark Propagator

The Fourier set of the Dirac fields is chosen to be

$$\psi(q; x) = \frac{1}{\sqrt{2\pi}} u(p; \vec{r}) e^{-i\omega t}. \quad (2.1)$$

Here, the compact notation

$$\begin{aligned} x &= \{t, \vec{r}\} \\ q &= \{\omega, p\} = \{\omega, \nu, \kappa, \mu\} \end{aligned} \quad (2.2)$$

has been introduced. ω is a continuous energy parameter, unrelated to the eigenenergy of the quark, and ν, κ, μ are the radial, Dirac and magnetic quantum numbers respectively. $u(p; \vec{r})$ are the quark cavity modes which are derived in appendix B.1. The following expressions make use of this short hand notation, namely

$$\delta(q, q') = \delta(\omega, \omega') \delta_{\nu\nu'} \delta_{\kappa\kappa'} \delta_{\mu\mu'} \quad (2.3)$$

and

$$\sum_q = \sum_{\nu\kappa\mu} \int_{-\infty}^{+\infty} d\omega. \quad (2.4)$$

This allows the orthonormality and completeness properties, showing the Dirac indices α and β explicitly, to be written as

$$\sum_{\alpha} \int d^4x \psi_{\alpha}^{\dagger}(q; x) \psi_{\alpha}(q'; x) = \delta(q, q') \quad (2.5)$$

$$\sum_q \psi_{\alpha}(q; x) \psi_{\beta}^*(q; x') = \delta^4(x, x') \delta_{\alpha\beta}. \quad (2.6)$$

For x inside the cavity, ψ must satisfy

$$(i \not{\partial} - m) \psi(q; x) = (\omega - \epsilon_p) \gamma^0 \psi(q; x). \quad (2.7)$$

The Feynman propagator in the cavity must satisfy

$$(i \not{\partial}_x - m) S(x, x') = \delta^4(x, x') \quad (2.8)$$

subject to the M.I.T. boundary condition

$$(i \vec{\gamma} \cdot \hat{r} + 1) S(x, x')|_{r=R} = 0. \quad (2.9)$$

where R is the radius of the cavity. Thus the Feynman propagator can be written as

$$S(x, y) = \sum_q \frac{\psi(q; x) \bar{\psi}(q; y)}{(\omega - \epsilon_p \pm i0)}, \quad (2.10)$$

where the $\pm i0$ or Feynman prescription, indicates that right hand poles are displaced downwards and left hand poles are shifted upwards in the complex ω -plane. Fourier transforming this into momentum space, ie.

$$S(q, q') = \int d^4x d^4y \bar{\psi}(q; x) \gamma^0 S(x, y) \gamma^0 \psi(q'; y), \quad (2.11)$$

the form which shall be used extensively

$$S(q, q') = \delta(q, q') \frac{1}{(\omega - \epsilon_p \pm i0)}, \quad (2.12)$$

is obtained.

2.2 Gluon Propagator

This section proceeds in a similar fashion to the previous section. This time the labels used are

$$q = \{w, p\} = \{w, N, J, M\} \quad (2.13)$$

and Σ , which is the polarization. The Fourier set for the vector fields are chosen to be

$$A^\mu(\Sigma, q; x) = \frac{1}{\sqrt{2\pi}} a^\mu(\Sigma, p; \vec{r}) e^{-i\omega t}, \quad (2.14)$$

where $a^\mu(\Sigma, p; \vec{r})$ are the gluon cavity modes (see appendix B.2). $A^\mu(\Sigma, q; x)$ are solutions to the d'Alembert equation subject to the M.I.T. boundary conditions. The orthogonality and completeness relations of these vector fields are

$$\int d^4x g^{\mu\nu} A_\mu^*(\Sigma, q; x) A_\nu(\Sigma', q'; x) = g^{\Sigma\Sigma'} \delta(q, q') \quad (2.15)$$

$$\sum_{\Sigma q} g^{\Sigma\Sigma} A^{*\mu}(\Sigma, q; x) A^\nu(\Sigma, q; x') = g^{\mu\nu} \delta(x, x'). \quad (2.16)$$

The gluon propagator (in the Feynman gauge) is defined by

$$D^{\mu\nu}(x, y) = - \sum_{\Sigma q} g^{\Sigma\Sigma} \frac{A^\mu(\Sigma, q; x) A^{\nu*}(\Sigma, q; y)}{(\omega^2 - \Omega_{\Sigma p}^2 + i0)}. \quad (2.17)$$

The relation

$$\square A^\mu(\Sigma, q; x) = -(\omega^2 - \Omega_{\Sigma p}^2) A^\mu(\Sigma, q; x), \quad (2.18)$$

which holds for all x inside the cavity, also holds true. Thus the gluon propagator satisfies

$$\square D_{\mu\nu}(x, y) = g_{\mu\nu} \delta(x, y). \quad (2.19)$$

After Fourier transforming the gluon propagator, the form that will be used extensively is

$$D^{\Sigma\Sigma'}(q, q') = - \frac{g^{\Sigma\Sigma'} \delta(q, q')}{(\omega^2 - \Omega_{\Sigma p}^2 + i0)}. \quad (2.20)$$

2.3 Fourier transform of $(\not{\not{p}} - 4m)$

In this section the Fourier transform of $(\not{\not{p}} - 4m)$ into momentum space is evaluated. The Fourier transform of $(\not{\not{p}} - m)$ is given by Stoddart [7]:

$$\int d^3r \bar{u}(p'; \vec{r}) (\not{\not{p}} - m) u(p; \vec{r}) = \delta(p', p) (\omega - \epsilon_p). \quad (2.21)$$

Using the cavity modes in appendix B.1, the following expression is calculated:

$$\int d^3r \bar{u}(p'; \vec{r}) u(p; \vec{r}) = \left(\frac{2mR(\kappa + \epsilon_p R) + \epsilon_p R}{2\epsilon_p R(\epsilon_p R + \kappa) + mR} \right) \quad (2.22)$$

so therefore the Fourier transform required is

$$\begin{aligned} \int d^3r \bar{u}(p'; \vec{r}) (\not{p} - 4m) u(p; \vec{r}) &= \delta(p', p) (\omega - \epsilon_p) \\ &- 3m \left(\frac{2mR(\kappa + \epsilon_p R) + \epsilon_p R}{2\epsilon_p R(\epsilon_p R + \kappa) + mR} \right). \end{aligned} \quad (2.23)$$

Chapter 3

Calculation of Quark Self-Energy in Free Space

In this section, an expression for Σ^0 using the Feynman rules is obtained. This integral is then regularized using the dimensional regularization technique and finally two appropriate renormalization schemes are investigated. This calculation has also been done by Pascual and Tarrach [11] amongst others. Pascual and Tarrach's approach is fairly similar to ours and yields a result consistent with ours. The major difference is that their prescription of D differs by a sign, namely, their D is given by $D = 4 + 2\epsilon$.

3.1 The Feynman Diagram

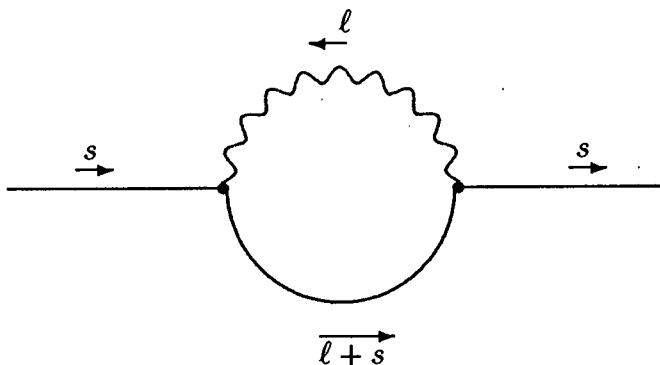


Figure 3.1: The Quark Self-Energy Feynman diagram in momentum space.

Using the Feynman rules, the expression for the quark self-energy is written in co-ordinate space as

$$-i\Sigma^0(x, y) = C(-ig\nu^\epsilon\gamma_\alpha)iS(x, y)(-ig\nu^\epsilon\gamma_\beta)iD^{\alpha\beta}(x, y), \quad (3.1)$$

where $C = 4 / 3$ is a colour factor and ν is an arbitrary mass scale required to make the coupling constant g dimensionless. $(-ig\nu^\epsilon\gamma_\alpha)$ is the vertex contribution, $S(x, y)$ is the quark propagator and $D^{\alpha\beta}(x, y)$ the gluon propagator. After Fourier transforming eq.(3.1) into momentum space, by integrating over the loop momenta, the result

$$-i\Sigma^0(\not{s}) = C \int \frac{d^D\ell}{(2\pi)^D} (-ig\nu^\epsilon\gamma_\alpha)iS(\not{s} + \not{\ell})(-ig\nu^\epsilon\gamma_\beta)iD^{\alpha\beta}(\not{\ell}) \quad (3.2)$$

is obtained. After inserting the propagators, the expression

$$\Sigma^0(\not{s}) = Cg^2\nu^{2\epsilon} \int \frac{d^D\ell}{(2\pi)^D} \frac{\gamma_\alpha(\not{s} + \not{\ell} + m)\gamma^\alpha}{((\ell + s)^2 - m^2)\ell^2} \quad (3.3)$$

is found. Extending the Clifford algebra into D dimensions, the gamma matrix identities derived in appendix A.1 are obtained. This allows $\Sigma^0(\not{s})$ to be simplified to

$$\Sigma^0(\not{s}) = Cg^2\nu^{2\epsilon} \int \frac{d^D\ell}{(2\pi)^D} \frac{(2 - D)(\not{s} + \not{\ell}) + Dm}{((\ell + s)^2 - m^2)\ell^2}. \quad (3.4)$$

This expression is in a form now ready to be regularized.

3.2 Regularization

In order to be able to evaluate the above integral, the following two Feynman integrals will have to be evaluated using the dimensional regularization scheme. Written compactly, these are

$$\{B, C^\mu\} = \nu^{2\epsilon} \int \frac{d^D\ell}{(2\pi)^D} \frac{\{1, \ell^\mu\}}{((\ell + s)^2 - m^2)\ell^2}. \quad (3.5)$$

Since these integrals are evaluated using the same techniques, only B is evaluated. The results of C^μ are quoted only, but can readily be verified. As an illustration of this technique, a much simpler Feynman integral has been evaluated in [SV]. Firstly note that B is written in Minkowski space. This

integral is converted into Euclidean space by the transformation discussed in appendix A.2, ie.

$$B = \nu^{2\epsilon} \int \frac{i d^D \ell}{(2\pi)^D} \frac{1}{(-(\ell + s)^2 - m^2)(-\ell^2)}. \quad (3.6)$$

The next step is to raise the denominator to exponential factors using

$$\frac{1}{(\ell + s)^2 + m^2} = \int_0^\infty dt_1 e^{-[(\ell+s)^2+m^2]t_1} \quad (3.7)$$

$$\frac{1}{\ell^2} = \int_0^\infty dt_2 e^{-\ell^2 t_2} \quad (3.8)$$

so that

$$B = i\nu^{2\epsilon} \int \frac{d^D \ell}{(2\pi)^D} \int_0^\infty dt_1 \int_0^\infty dt_2 e^{-[(\ell+s)^2 t_1 + m^2 t_1 + \ell^2 t_2]}. \quad (3.9)$$

At this stage, the integral is in a form that is very similar to the Gaussian integrals, namely

$$\int_{-\infty}^\infty \frac{d^D \ell}{(2\pi)^D} \{1, \ell, \ell^2\} e^{-\ell^2 z} = \left\{1, 0, \frac{1}{2z}\right\} \left(\frac{1}{4\pi z}\right)^{D/2}. \quad (3.10)$$

The difference is that there is a term in the exponent of eq.(3.9) linear in ℓ . This is simply eliminated by introducing the required shift of variables, namely

$$\ell' = \ell + \frac{st_1}{t_1 + t_2} = (\ell + s) - \frac{st_2}{t_1 + t_2}. \quad (3.11)$$

This integral must be converted into the z -form. Since the original expression contains two denominators, B has ended up with two infinite integrals, namely, the t_1 and t_2 integrals. Combining these integrals by using the change of variables

$$\begin{aligned} t_1 &= zt \\ t_2 &= z(1-t), \end{aligned} \quad (3.12)$$

leaves us with one integral from 0 to ∞ , namely the z integral. The other integral, the t integral, is from 0 to 1. Thus, using eq.'s(3.10)–(3.12) and after some manipulation, B in the z -form is

$$B = \frac{i}{(4\pi)^2} \left(\frac{1}{4\pi\nu^2}\right)^{-\epsilon} \int_0^\infty dz z^{-1+\epsilon} \int_0^1 dt e^{-[s^2(1-t)+m^2]zt}. \quad (3.13)$$

This z -integral is in the form of the Gamma functions (appendix A.4)

$$B = \frac{i}{(4\pi)^2} \left(\frac{1}{4\pi\nu^2} \right)^{-\epsilon} \int_0^1 dt [s^2 t(1-t) + m^2 t]^{-\epsilon} \Gamma(\epsilon). \quad (3.14)$$

By expanding the integrand to $O(\epsilon)$ using $[x]^{-\epsilon} = 1 - \epsilon \ln[x] + O(\epsilon^2)$ and using the expansion of $\Gamma(\epsilon)$ for small ϵ (appendix A.4) the following expression is obtained:

$$B = \frac{i}{(4\pi)^2} \left(\frac{1}{4\pi\nu^2} \right)^{-\epsilon} \int_0^1 dt \left[\frac{1}{\epsilon} - \gamma - \ln((s^2(1-t) + m^2)t) \right] + O(\epsilon). \quad (3.15)$$

This integral is of the form of the K and L functions found in appendix A.3. The result, which has been converted back into Minkowski space, is

$$B = \frac{i}{(4\pi)^2} \left[\frac{1}{\epsilon} - \gamma - \ln \left(\frac{m^2}{4\pi\nu^2} \right) + 2 - \left(1 - \frac{m^2}{s^2} \right) \ln \left(1 - \frac{s^2}{m^2} \right) \right]. \quad (3.16)$$

The other integral is given by

$$C^\mu = \frac{-is^\mu}{(4\pi)^2} \left(\frac{1}{4\pi\nu^2} \right)^{-\epsilon} \int_0^\infty dz z^{-1+\epsilon} \int_0^1 dt t e^{-[s^2(1-t)+m^2]zt} \quad (3.17)$$

in Euclidean space. The final result in Minkowski space is

$$C^\mu = \frac{-is^\mu}{2(4\pi)^2} \left[\frac{1}{\epsilon} - \gamma - \ln \left(\frac{m^2}{4\pi\nu^2} \right) + 2 - \frac{m^2}{s^2} - \left(1 - \frac{m^2}{s^2} \right)^2 \ln \left(1 - \frac{s^2}{m^2} \right) \right]. \quad (3.18)$$

The final result of the self energy, after using these Feynman Integrals, in Minkowski space, is

$$\begin{aligned} \Sigma^0(\not{s}) &= \frac{\alpha_s}{3\pi} \left[(4m - \not{s}) \left(\frac{1}{\epsilon} - \gamma - \ln \left(\frac{m^2}{4\pi\nu^2} \right) \right) \right. \\ &\quad + 4m \left(\frac{3}{2} - \left(1 - \frac{m^2}{s^2} \right) \ln \left(1 - \frac{s^2}{m^2} \right) \right) \\ &\quad \left. - \not{s} \left(\left(1 + \frac{m^2}{s^2} \right) - \left(1 - \frac{m^4}{s^4} \right) \ln \left(1 - \frac{s^2}{m^2} \right) \right) \right]. \quad (3.19) \end{aligned}$$

3.3 Renormalization

Two different renormalization schemes are investigated. The first scheme is the minimal subtraction scheme (ms). This scheme involves a simple subtraction of the term proportional to $\Gamma(\epsilon)$. The second scheme is included in order to make comparisons with Goldhaber, Hansson and Jaffe [5, 6] (hereafter referred to as [GHJ]) results. This scheme includes an extra finite piece in the subtraction factor and is an amended mass renormalization scheme (\overline{ms}). Cheng and Li [12] and Nash [13] provide further elaboration on these and other renormalization schemes.

3.3.1 Minimal Subtraction Scheme

Noting that the form of $\Gamma(\epsilon)$, is

$$\Gamma(\epsilon) = \int_0^\infty dz z^{-1+\epsilon} e^{-z} = \frac{1}{\epsilon} - \gamma + O(\epsilon) \quad (3.20)$$

allows the term proportional to $\Gamma(\epsilon)$ to be selected, by inspection, as the subtraction factor. Looking at eq.(3.19), the integrand of this factor is found to be

$$S(z) = \frac{\alpha_s}{3\pi} (4m - \not{s}) z^{-1+\epsilon} e^{-z}. \quad (3.21)$$

Using the Fourier transform of $(\not{s} - 4m)$, eq.(2.23), the subtraction factor is obtained for use in cavity space. This expression is now in the form which is used computationally.

3.3.2 Mass Renormalization Scheme

In this section, a comparison is made between the approach of [GHJ]'s to our approach. [GHJ]'s result of Σ^0 using the Pauli-Villars regularization scheme and after evaluating their integral is

$$\begin{aligned} \Sigma_{Gold}^0 = & \frac{\alpha_s}{3\pi} \left\{ (\not{s} - 4m) [\ln m^2 - \ln \Lambda^2] \right. \\ & + 4m \left[1 - \left(1 - \frac{m^2}{s^2} \right) \ln \left(1 - \frac{s^2}{m^2} \right) \right] \\ & \left. - \not{s} \left[\frac{3}{2} + \frac{m^2}{s^2} - \left(1 - \left(\frac{m^2}{s^2} \right)^2 \right) \ln \left(1 - \frac{s^2}{m^2} \right) \right] \right\}. \quad (3.22) \end{aligned}$$

We¹ start off by imposing the condition

$$\Sigma_{Gold}^0|_{\not{s}=m} - \Sigma^0|_{\not{s}=m} = 0 \quad (3.23)$$

in order to obtain a relation between [GHJ]'s cut-off point, $\ln \Lambda^2$, and the pole $1/\epsilon$. This yields

$$\frac{\alpha_s}{3\pi} \left[-3m \left(-\ln \Lambda^2 + \frac{1}{\epsilon} - \gamma + \ln 4\pi\nu^2 + \frac{5}{6} \right) \right] = 0. \quad (3.24)$$

In other words

$$\ln \Lambda^2 = \frac{1}{\epsilon} - \gamma + \ln 4\pi\nu^2 + \frac{5}{6}. \quad (3.25)$$

This equation is valid for a particular ν only. This particular value is found in section 4.4. The free space quark propagator is expanded as

$$\begin{aligned} iS(\not{s}) &= \frac{i}{\not{s}-m} + \frac{i}{\not{s}-m} [-i\Sigma^0(\not{s})] \frac{i}{\not{s}-m} + \\ &\quad \frac{i}{\not{s}-m} [-i\Sigma^0(\not{s})] \frac{i}{\not{s}-m} [-i\Sigma^0(\not{s})] \frac{i}{\not{s}-m} + \dots \end{aligned} \quad (3.26)$$

which can easily be verified to be

$$iS(\not{s}) = \frac{i}{\not{s}-m-\Sigma^0(\not{s})}. \quad (3.27)$$

The renormalized self-energy, Σ_R^0 , and an infinite quantity, Z_2 , are defined through the propagator via the definition of the renormalized mass, namely from the relation

$$\frac{i}{\not{s}-m-\Sigma^0(\not{s})} = \frac{iZ_2}{\not{s}-m_R-\Sigma_R^0(\not{s})}. \quad (3.28)$$

[GHJ] defines the renormalized mass by introducing a renormalization point μ . Their renormalized mass is

$$m_R = m + \frac{\alpha_s}{\pi} m \ln \left(\frac{\Lambda^2}{\mu^2} \right). \quad (3.29)$$

By rewriting the inverse propagator in terms of the quantities defined in eq.(3.29) and eq.(3.25) and using the expression obtained for Σ^0 , eq.(3.19),

¹see [14].

the renormalized self-energy is given as

$$\begin{aligned} \Sigma_R^0 = & \frac{\alpha_s}{3\pi} \left\{ (\not{s} - 4m_R) \ln \frac{1}{\mu^2} \right. \\ & + 4m_R \left(\frac{2}{3} - \left(1 - \frac{m_R^2}{s^2} \right) \ln \left(1 - \frac{s^2}{m_R^2} \right) - \ln m_R^2 \right) \\ & \left. - \not{s} \left(\frac{1}{6} + \frac{m_R^2}{s^2} - \left(1 - \frac{m_R^4}{s^4} \right) \ln \left(1 - \frac{s^2}{m_R^2} \right) - \ln m_R^2 \right) \right\}. \end{aligned} \quad (3.30)$$

which includes [GHJ]'s parameter μ . To find the corresponding subtraction factor, the relation

$$\Sigma_R^0 = \Sigma^0 - S \quad (3.31)$$

is used. From eq.(3.19) and eq.(3.30)

$$\Sigma^0 - \Sigma_R^0 = S = \frac{\alpha_s}{3\pi} (4m - \not{s}) \left(\frac{1}{\epsilon} - \gamma + \ln 4\pi\nu^2 + \frac{5}{6} - \ln \mu^2 \right) \quad (3.32)$$

which, by using eq.(3.25), is

$$S = \frac{\alpha_s}{3\pi} (4m - \not{s}) \left(\ln \left(\frac{\Lambda^2}{\mu^2} \right) \right) \quad (3.33)$$

as expected. For the case $\ln \mu^2 = 5/6$, eq.(3.32) reduces to the usual mass renormalization scheme ($\overline{m\overline{s}}$). Note the similarities between eq.(3.32) and eq.(3.21). This expression will also be taken directly to the computer.

Chapter 4

Calculation of Quark Self-Energy in a cavity

In this chapter, the calculation of the quark self-energy in a cavity, using the cavity propagators outlined in chapter 2, is performed. The renormalization discussion, which was initiated in the previous chapter, is followed through to the cavity. A comparison between our results and [GHJ]'s results is made.

4.1 Calculation of Σ^C

The calculation of Σ^C closely follows the technique used to calculate Σ^0 , as outlined in section 3.1. We start off with the expression obtained from the Feynman diagram

$$-i\Sigma^C(x, y) = C(-ig\nu^\epsilon\gamma_\alpha)iS(x, y)(-ig\nu^\epsilon\gamma_\beta)iD^{\alpha\beta}(x, y). \quad (4.1)$$

Using the cavity propagators, which have been Fourier transformed into cavity space, and the compact notation for the spatial overlap integrals, which is outlined in appendix C.1, the result obtained is

$$\Sigma^C(\omega, p, p') = ig^2C \int_{-\infty}^{\infty} \frac{d\omega_2}{2\pi} \sum_{p_1 p_2 \Sigma} g^{\Sigma\Sigma} Q_{pp_1}^{\Sigma p_2} \tilde{Q}_{p_1 p'}^{\Sigma p_2} \times \frac{\omega - \omega_2 + \epsilon_{p_1}}{((\omega - \omega_2)^2 - \epsilon_{p_1}^2 + i0)} \frac{1}{(\omega_2^2 - \Omega_{p_2}^2 + i0)}. \quad (4.2)$$

Σ and p_2 label the intermediate gluon and p_1 labels the intermediate quark. Evaluating the ω_2 integral, a series form for the self-energy is obtained,

$$\Sigma^C(\omega, p, p) = \alpha_s C \sum_{p_1 p_2 \Sigma} M(p_1, p_2, \Sigma) \frac{1}{2\Omega_{p_2}[\omega - \text{sgn}(\epsilon_{p_1})\Omega_{p_2} - \epsilon_{p_1}]}. \quad (4.3)$$

Here, the vertex factor

$$M(p_1, p_2, \Sigma) = \sum_{\mu_2 M_2} 4\pi g^{\Sigma\Sigma} Q_{pp_1}^{\Sigma p_2} \tilde{Q}_{p_1 p'}^{\Sigma p_2} \quad (4.4)$$

has been introduced. To obtain the z -form from eq.(4.2), the denominators are evaluated as before, namely

$$\Sigma^C(\omega, p, p') = \alpha_s C \int_0^\infty dz \sum_{p_1 p_2 \Sigma} M(p_1, p_2, \Sigma) K(p_1, p_2, \Sigma; z), \quad (4.5)$$

where

$$K(p_1, p_2, \Sigma; z) = i^2 z^{1/2} \int_0^1 dt \frac{1}{\sqrt{4\pi}} (\omega t + \epsilon_{p_1}) e^{z[\omega^2 t(1-t) - \epsilon_{p_1}^2 (1-t) - \Omega_{\Sigma p_2}^2 t]}. \quad (4.6)$$

The above summation, eq.(4.3), will diverge or converge very slowly for large z if the condition, $[\omega^2 t(1-t) - \epsilon_{p_1}^2 (1-t) - \Omega_{\Sigma p_2}^2 t] > -1$, is satisfied. In this case, the expression eq.(4.3) is used instead of eq.(4.6). Eq.(4.3) is also a useful test of eq.(4.6) for ω satisfying the above inequality.

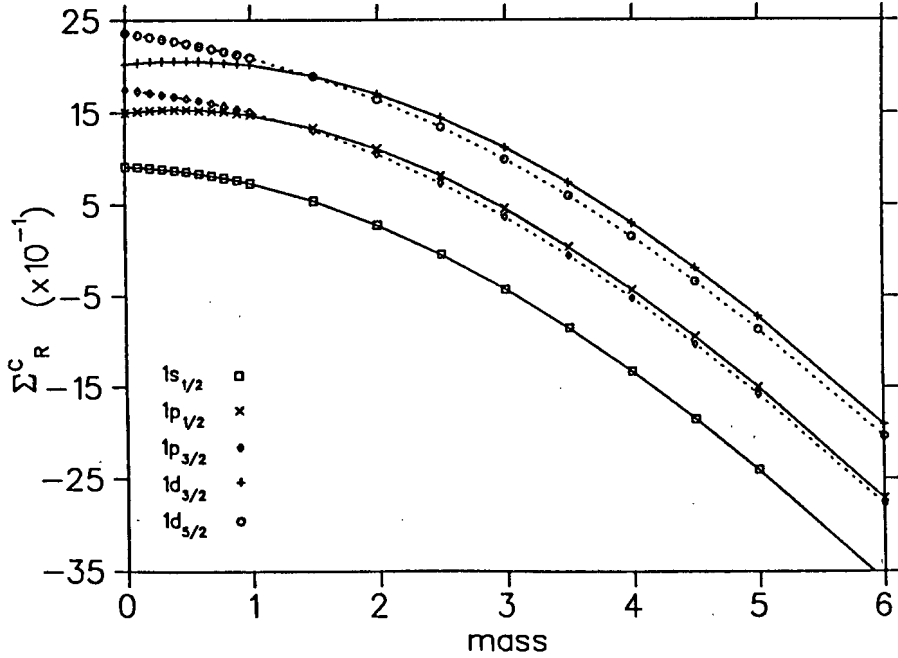


Figure 4.1: Self-Energy of the quark for external cavity modes $\nu = 1$

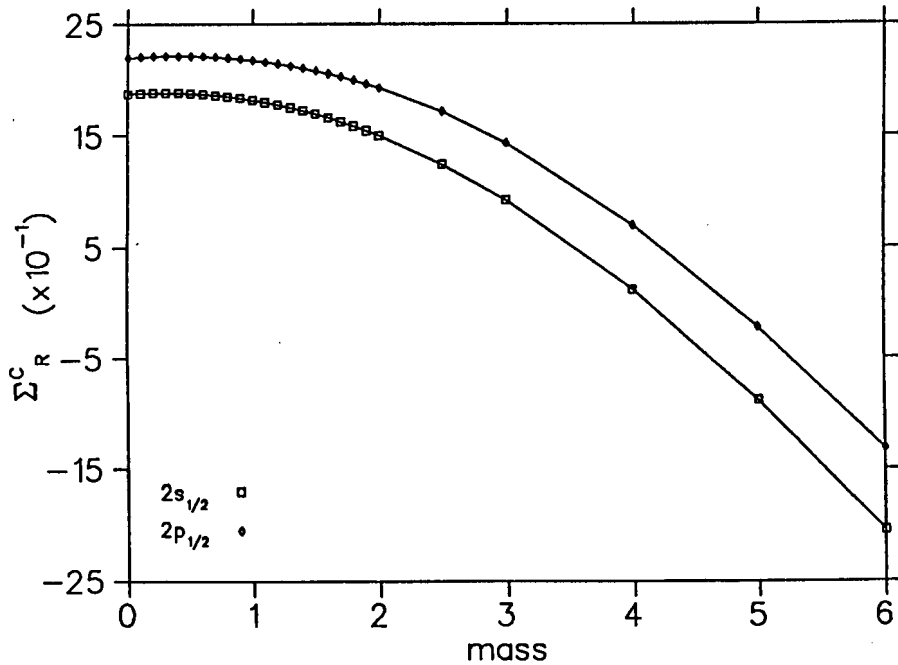


Figure 4.2: Self-Energy of the quark for external cavity modes $\nu = 2$

4.2 Minimal Subtraction Scheme

The \overline{ms} scheme is trivial. Both $\Sigma^C(\epsilon = 0, z)$ and $S(\epsilon = 0, z)$ have now been found so the diagonal terms of $\Sigma_R^C(p, p')$ can be computed. This has been done for $\nu = 1, 2$ which have been plotted in figures 4.1 and 4.2. A pole in ω results, if the energy conservation relation,

$$\omega - \Omega_{p_2} - \epsilon_{p_1} = 0, \quad (4.7)$$

is satisfied for any states in the summation over the internal quantum states. These particular contributions have been removed from the quoted results and are investigated in the following section.

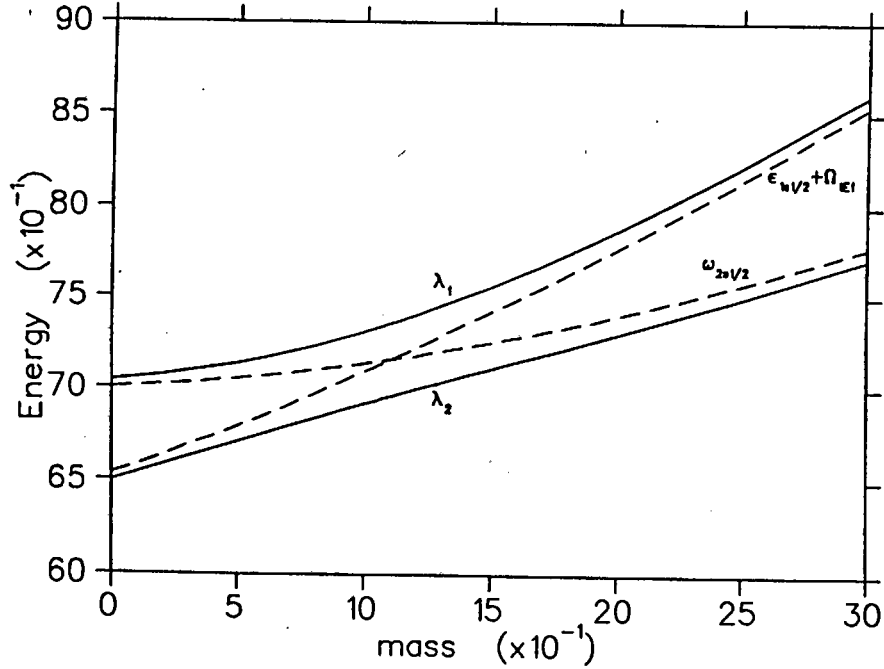


Figure 4.3: Eigenenergies of the $|q\rangle$, $|qg\rangle$ states.

4.3 Energy Conservation

Note the pole in ω that results from the factor $[\omega - \text{sgn}(\epsilon_{p_1})\Omega_{p_2} - \epsilon_{p_1}]^{-1}$ in eq.(4.3). Since the calculation is only being done for the on shell scheme, $\omega > 0$. In the specific case of $\epsilon_{p_1} < 0$, the denominator can be written as $[\omega + \Omega_{p_2} + |\epsilon_{p_1}|]^{-1}$, which is positive definite. In other words, there is no pole for $\epsilon_{p_1} < 0$, however, by the same token, there definitely is a pole for $\epsilon_{p_1} > 0$.

In figure 4.3, particular eigenenergies that have been determined to 'cause' a pole are plotted. For the moment, ignore the solid lines. The dashed lines are the eigenenergies, as a function of the quark mass, of firstly, the external quark ($\omega_{2p_{1/2}}$) and secondly, the sum of the intermediate quark and gluon ($\epsilon_{1s_{1/2}} + \Omega_{1E_1}$). One can see that these two eigenenergies are equal at some particular mass. This results in the denominator of eq.(4.3) being zero. In figure 4.4, the $2p_{1/2}$ self-energy graph is shown as the dashed line. Here, the effect of the pole can clearly be seen. The dotted line is the contribution due to the quark self-energy graph by the state of incoming quark $2p_{1/2}$, internal quark $1s_{1/2}$ and gluon $1E_1$. The straight line is the quark self-energy with this particular state removed. In other words the pole results from this state only.

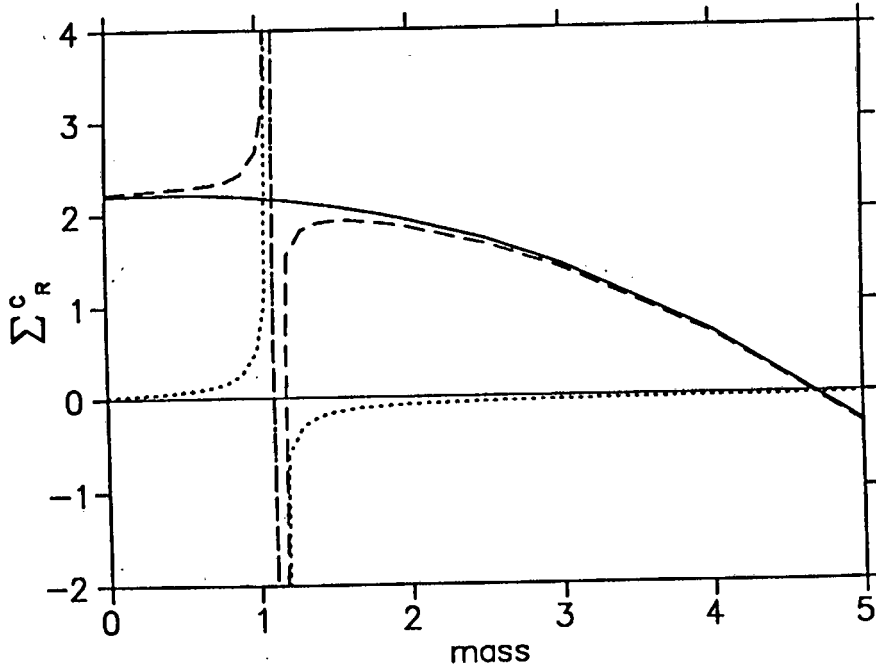


Figure 4.4: The Quark Self-Energy of external cavity mode $\nu = 2, \kappa = 1$.

Let us investigate what is happening here. The emission of a gluon from a quark is permitted provided that, either, the gluon is reabsorbed within a short period of time by the original quark, such that it satisfies Heisenberg's uncertainty principle, or, the energy of the original quark state is the same as that of the final quark-gluon state. In other words energy is conserved and the gluon may not necessarily be reabsorbed by the original quark. If the later is the case then

$$\omega - \Omega_{p_2} - \epsilon_{p_1} = 0. \quad (4.8)$$

This is exactly the form of the denominator of eq.(4.3) for $\epsilon_{p_1} > 0$ at the pole. For the particular states that the energy conservation equation above is satisfied, a mixture of the quark self-energy with another $O(g^2)$ diagram occurs. This $O(g^2)$ diagram contains two quark-gluon vertices which, unlike the quark self-energy, require energy conservation before and after each vertex.

Making use of time independent perturbation theory (eg. see Migdal [15]), the coupling of the two states, which are represented by $|q\rangle$ and $|qg\rangle$, are investigated. These states are the incoming quark state and the mixed state of the intermediate quark and gluon respectively. If there are no interac-

tions between the two states, the eigenenergies are given by the unperturbed Hamiltonian

$$\begin{aligned} H_0|q\rangle &= \omega|q\rangle \\ H_0|qg\rangle &= (\epsilon_{p_1} + \Omega_{p_2})|qg\rangle. \end{aligned} \quad (4.9)$$

The eigenvalues of these equations are plotted as dotted lines in figure 4.3. The perturbation is due to the interaction term which is written as

$$H_1 = \begin{pmatrix} 0 & V(|q\rangle \rightarrow |qg\rangle) \\ V(|q\rangle \rightarrow |qg\rangle) & 0 \end{pmatrix}. \quad (4.10)$$

The eigenvalues and eigenvectors of the perturbed Hamiltonian are found by solving

$$H|Q_{1,2}\rangle = (H_0 + H_1)|Q_{1,2}\rangle = \lambda_{1,2}|Q_{1,2}\rangle, \quad (4.11)$$

where the eigenvectors are given in terms of the original states by

$$\begin{aligned} |Q_1\rangle &= c_{11}|q\rangle + c_{12}|qg\rangle \\ |Q_2\rangle &= c_{21}|q\rangle + c_{22}|qg\rangle. \end{aligned} \quad (4.12)$$

After diagonalising the Hamiltonian, the following results are found:

$$\begin{aligned} \lambda_1 &= \omega + \frac{4\pi\alpha_s V(|q\rangle \rightarrow |qg\rangle)^2}{\omega - \epsilon_{p_1} - \Omega_{p_2}}, \\ \lambda_2 &= \epsilon_{p_1} + \Omega_{p_2} - \frac{4\pi\alpha_s V(|q\rangle \rightarrow |qg\rangle)^2}{\omega - \epsilon_{p_1} - \Omega_{p_2}}, \end{aligned} \quad (4.13)$$

where the interaction potential is found to be

$$V(|q\rangle \rightarrow |qg\rangle)^2 = \frac{CM(\omega, \epsilon_{p_1}, \Omega_{p_2})}{8\pi\Omega_{p_2}}. \quad (4.14)$$

The eigenenergies λ_1 and λ_2 are plotted as solid lines in figure 4.3. In this figure, $\alpha_s = 2.2$ has been used. Bear in mind that λ_1 and λ_2 are exact solutions and the calculation of the self-energy has been done only up to $O(\alpha_s)$. The expansion of λ_1, λ_2 to $O(\alpha_s)$, in any case, appears to have the identical pole as the quark self-energy since the expansion of the λ 's near the pole is divergent. This particular contribution to the self-energy will simply be excluded.

These poles have not been found for the very low cavity modes calculated up to $mass = 10$, but have been found for the higher cavity modes. There are too many poles in the states higher than $2p_{1/2}$ for the results to be meaningful.

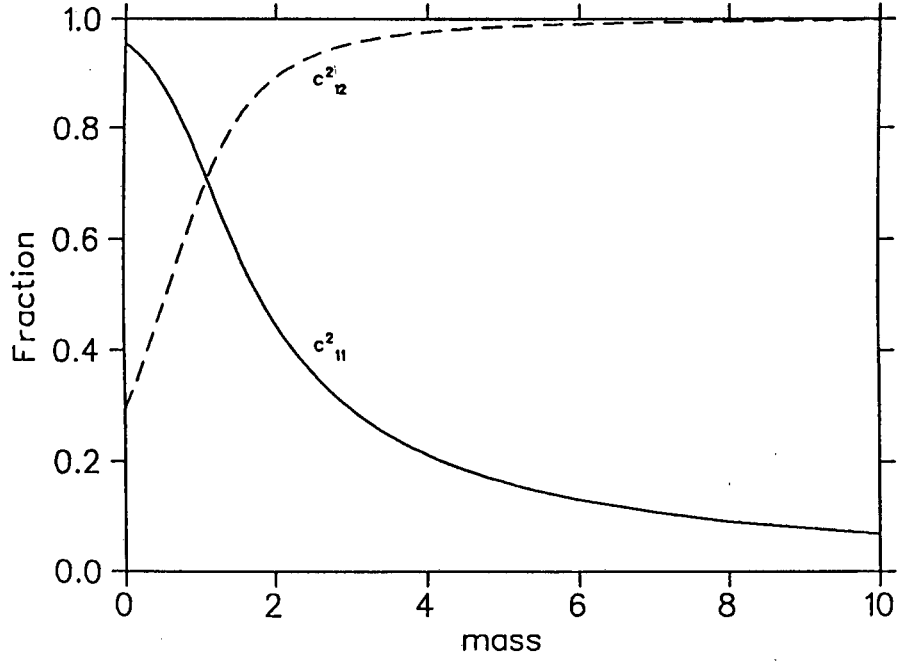


Figure 4.5: The coefficients of vector $|Q_1\rangle$'s components.

The square of the normalized coefficients describes the mixture of the $|q\rangle$ and $|qq\rangle$ states. For simplification, the following variables have been defined

$$m = \frac{\omega - \epsilon_{p_1} - \Omega_{p_2}}{2}$$

$$p = \frac{\sqrt{(\omega - \epsilon_{p_1} - \Omega_{p_2})^2 + 16\pi\alpha_s V(|q\rangle \rightarrow |qq\rangle)^2}}{2}. \quad (4.15)$$

This allows the normalized coefficients to be written as

$$c_{11} = \sqrt{\frac{4\pi\alpha_s V^2}{4\pi\alpha_s V^2 + m^2 - 2mp + p^2}}$$

$$c_{12} = \frac{-m + p}{\sqrt{4\pi\alpha_s V^2 + m^2 - 2mp + p^2}}$$

$$c_{21} = \sqrt{\frac{4\pi\alpha_s V^2}{4\pi\alpha_s V^2 + m^2 + 2mp + p^2}} = c_{12}$$

$$c_{22} = \frac{-m - p}{\sqrt{4\pi\alpha_s V^2 + m^2 + 2mp + p^2}} = -c_{11}. \quad (4.16)$$

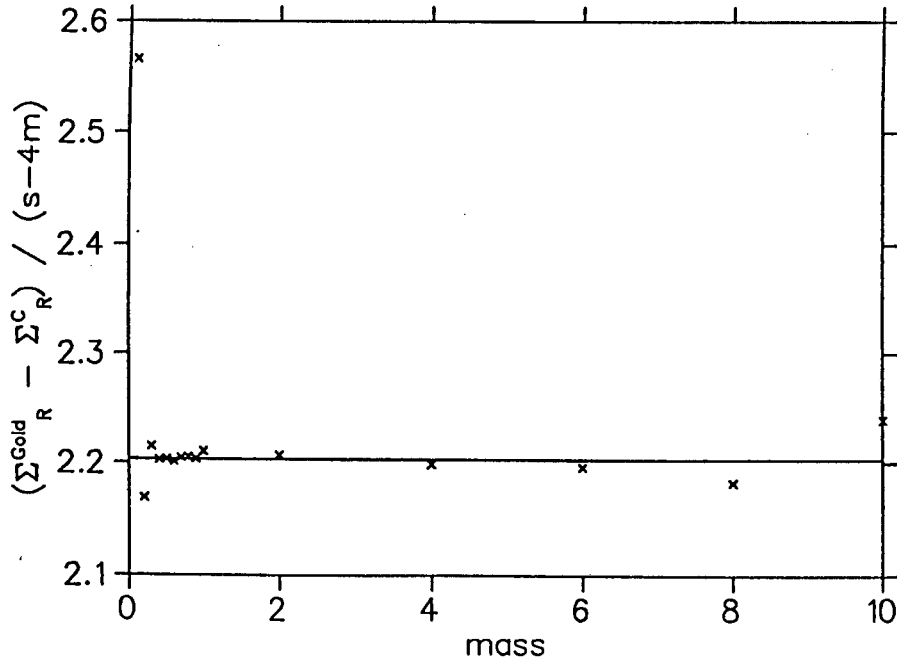


Figure 4.6: Graph to determine the renormalization parameter ν

In figure 4.5, the square of the normalized coefficients of λ_1 are plotted. c_{11} is the coefficient of the dressed quark $|q\rangle$, c_{12} is the coefficient of the dressed quark-gluon state $|qg\rangle$ which implies that c_{11}^2 is the self-energy fraction of λ_1 and c_{12}^2 is quark-gluon state fraction of λ_1 .

4.4 Mass Renormalization Scheme

In this section, the differences between our results and [GHJ]'s results are established, by calculating the scale parameter ν .

Referring back to section 3.3.2, the subtraction factor is seen to be dependent on two scale parameters, μ and ν . Pauli-Villars regularization, used by [GHJ], introduces a parameter which has been labeled μ . ν is the parameter related to dimensional regularization and in general includes the μ parameter. However, for simplicity, these constants are kept separate since the form of μ is known. In other words the μ dependence in both ours and [GHJ]'s result are identical and ν is the constant of proportionality between the two scale parameters. [GHJ] have written their final results as

$$\Sigma_{\text{Gold}} = \Sigma^1 + \ln(\mu^2)\Sigma^2 + \tilde{\Sigma}. \quad (4.17)$$

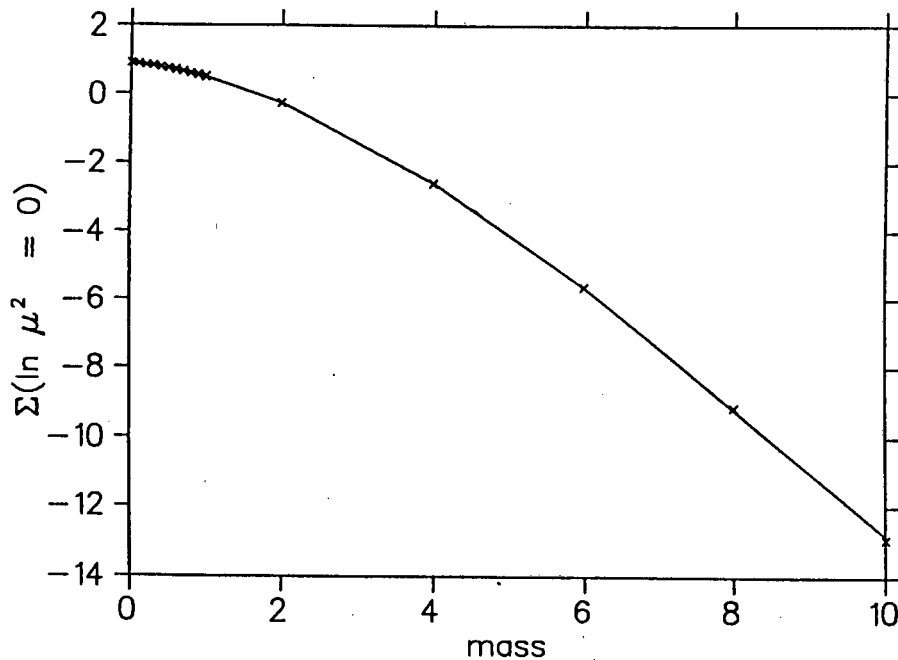


Figure 4.7: Comparison of results. The points are found using [GHJ]'s results directly. Our results are given by the curve.

The μ dependence part can be extracted and is equal to

$$\frac{\alpha_s}{3\pi}(4m - \not{s}) = \Sigma^2. \quad (4.18)$$

To find the appropriate ν , the μ dependence from our $\Sigma^C(\nu, \mu)$ and $\Sigma_{Gold}^C(\mu)$ is eliminated and then the difference between the two results is found. Since [GHJ]'s result has had all scale dependence removed, the value of ν is fixed. The difference with the factor $(\not{s} - 4m)$ removed is plotted as a function of mass in figure 4.6. By calculating the best fit through these points, the values of $-\ln \nu^2$ is obtained. This quantity cannot be calculated to high precision since [GHJ]'s results used are quoted to between two and four significant figures only.

From these results, $-\ln \nu^2 = 2.203 \pm 0.271$. Figure 4.7 shows the comparison between our results and [GHJ]'s. [GHJ]'s results are indicated by the crosses and our results by the curve.

4.5 Accuracy of Results

The calculation of Σ^C is identical to that done in [SV]. In [SV] a number of numerical checks were used to check Σ^C . These are also used here. In this section, certain elements of the calculation with respect to numerical checks and accuracy are outlined.

The accuracy of the eigenenergies are dependent on the Bessel functions which are used. With accurate numerical Bessel functions one can expect eigenenergies with up to 14 digit accuracy.

The vertex integrals are contained in the factor M and are checked using the qgg sum rule in appendix C.2 (eq.(C.15)). The agreement is dependent on the number of modes used in the sum. With 13 modes, agreement to 5 decimal places for low gluon cavity modes is obtained. In general, the summation in eq.(4.5) is suppressed by the exponential factor in eq.(4.6), and the accuracy of Σ^C is much higher.

The K function is made up of error functions for which if great care is taken, 14 digit accuracy can also be obtained. K is numerically checked by evaluating the z integral of eq.(4.5) for selected states of p_1 and p_2 and comparing the results obtained from eq.(4.3) for the same states. These selected states must, however, satisfy the inequality $[\omega^2 t(1-t) - \epsilon_{p_1}^2(1-t) - \Omega_{\Sigma p_2}^2 t] > -1$, otherwise the z -integral does not converge.

Σ^C is a summation over an infinite number of internal quantum states. At some stage this sum is cut off. The cut off point is chosen by limiting both the quark and gluon eigenenergies. The maximum energy E_{max} has been chosen to be between 40 and 50. An estimate of the error on Σ_R^C can be made by comparing $\Sigma_R^C(E_{max})$ and $\Sigma_R^C(E_{max} + \pi)$ since π is the approximate spacing between energy levels in a cavity. The heavier masses and higher external quark modes require higher eigenenergies in their sums. As a result, these tend to be the least accurate results.

At low z , Σ^C cannot be computed directly since two divergences are being subtracted numerically, namely

$$\Sigma_R^C = \int_0^\infty dz(\Sigma^C(0, z) - S(0, z)). \quad (4.19)$$

What is done here, is to use a six or seven degree polynomial fit on the integrand of the above equation, for some small range of z , close enough to 0 to be meaningful, yet not too close such that Σ^C and S are still reasonably accurate. This polynomial fit is then used for the 'missing' integrand. By doing a number of polynomial fits of, for example, six and seven degree

polynomials, over slightly different ranges, an average and an estimate of the error of the fit is obtained.

In the table below, Σ_R^C of the low lying cavity modes for $m = 10$ is calculated firstly using $E_{max} = 40$ then $E_{max} = 40 + \pi$. The last column is the error of the polynomial fit for the $E_{max} = 40$ value.

Cavity mode	$E_{max} = 40$	$E_{max} = 40 + \pi$	Polynomial error
$1s_{1/2}$	-9.375 193	-9.375 187	0.027 791
$1p_{1/2}$	-8.541 433	-8.541 417	0.028 330
$1p_{3/2}$	-8.569 866	-8.569 854	0.028 356
$1d_{3/2}$	-7.721 785	-7.721 758	0.030 075
$1d_{5/2}$	-7.789 701	-7.789 682	0.029 986
$2s_{1/2}$	-7.817 216	-7.817 188	0.033 119
$2p_{1/2}$	-6.973 182	-6.973 218	0.041 669

Here, four polynomials have been used, two of six degree and two of seven degree. As can be seen, Σ_R^C is changing in the fifth decimal place after $E_{max} = 40$. The Polynomial error can be reduced by taking more polynomial fits.

Chapter 5

Conclusion

In this thesis, we have successfully utilized the method of subtracting out divergences, developed in [SV], to calculate the massive quark self-energy in a cavity. The value of ν could not be determined with a high degree of accuracy so the results using the amended $\overline{m\bar{s}}$ renormalization scheme could not be obtained very accurately.

5.1 Acknowledgements

I would like to thank the Foundation for Research and Development for their financial support which made this thesis possible. My supervisor, Prof. R.D. Viollier deserves special thanks for his support and guidance throughout my M.Sc. I am grateful to Dr. A.J. Stoddart for introducing me to the techniques used in this thesis, both analytical and computational, Dr. G.B. Tupper for his help with the renormalization schemes. Dr. M.S. O'Connor deserves special recognition for, amongst other things, his endless computer services and extensive proofreading of this thesis. Dr. G.U. Schreiber deserves thanks for her help, especially with the self-energy diagram. I would lastly like to thank the students and staff of the Physics department for their general guidance and support of this thesis.

Appendix A

Mathematical appendices

In this appendix, a number of mathematical identities, which are commonly used in the main calculation, are presented.

A.1 Gamma Matrix Identities in D Dimensions

The Minkowski space metric

$$g^{\mu\nu} = g_{\mu\nu} = \text{diag}(1, -1, -1, -1) \quad (\text{A.1})$$

$$g_{\nu}^{\mu} = \delta_{\nu}^{\mu} \quad (\text{A.2})$$

and the 4×4 Dirac γ matrices which satisfy the Clifford algebra

$$\{\gamma^{\mu}, \gamma^{\nu}\} = 2g^{\mu\nu}. \quad (\text{A.3})$$

are used. Our calculations are performed in $D = 4 - 2\epsilon$ dimensions where ϵ is small. The dot product of two gamma matrices is extended into D-dimensions as

$$\gamma^{\mu} \gamma_{\mu} = D. \quad (\text{A.4})$$

Using the previous two equations it is easy to show that

$$\gamma^{\mu} \not{k} \gamma_{\mu} = (2 - D) \not{k}. \quad (\text{A.5})$$

A.2 Conversion to Euclidean Space

The metric in Minkowski space in general is

$$g^{\mu\nu} = g_{\mu\nu} = \text{diag}(1, -1, -1, \dots, -1) \quad (\text{A.6})$$

and in Euclidean space is

$$g^{\mu\nu} = g_{\mu\nu} = \text{diag}(1, 1, 1, \dots, 1). \quad (\text{A.7})$$

Let M^ν be an arbitrary Minkowski vector and E^ν , the converted Euclidean vector. So if

$$M^\nu = (m_0, m_1, m_2, \dots, m_{D-1}) \quad (\text{A.8})$$

then

$$E^\nu = (e_0, e_1, e_2, \dots, e_{D-1}) = (im_0, m_1, m_2, \dots, m_{D-1}). \quad (\text{A.9})$$

This means the invariant dot product is

$$M^2 = m_0^2 - m_1^2 - m_2^2 - \dots - m_{D-1}^2 \quad (\text{A.10})$$

$$\begin{aligned} E^2 &= e_0^2 + e_1^2 + e_2^2 + \dots + e_{D-1}^2 \\ &= -m_0^2 + m_1^2 + m_2^2 + \dots + m_{D-1}^2 \\ &= -M^2 \end{aligned} \quad (\text{A.11})$$

and thus the infinitesimal element is given by

$$d^D M = id^D K. \quad (\text{A.12})$$

A.3 Some Common Integrals

The following two integrals are used regularly, namely

$$K_n(q) = \int_0^1 dz z^n \ln(q - z) \quad (\text{A.13})$$

$$L_n(q) = \int_0^1 dz z^n \ln(q + z) \quad (\text{A.14})$$

for $n = 0, 1$. These integrals may be evaluated using

$$\int du \ln(u) = u \ln(u) - u \quad (\text{A.15})$$

and

$$\int du u \ln(u) = \frac{u^2}{2} \left(\ln(u) - \frac{1}{2} \right). \quad (\text{A.16})$$

The results are as follows,

$$K_0(q) = q \ln \left(\frac{q}{q-1} \right) + \ln(q-1) - 1 \quad (\text{A.17})$$

$$K_1(q) = \frac{q^2}{2} \ln \left(\frac{q}{q-1} \right) + \frac{1}{2} \ln(q-1) - \frac{q}{2} - \frac{1}{4} \quad (\text{A.18})$$

$$L_0(q) = q \ln \left(\frac{q+1}{q} \right) + \ln(q+1) - 1 \quad (\text{A.19})$$

$$L_1(q) = \frac{q^2}{2} \ln \left(\frac{q}{q+1} \right) + \frac{1}{2} \ln(q+1) + \frac{q}{2} - \frac{1}{4} \quad (\text{A.20})$$

and some special values

$$\begin{aligned} K_0(1) &= -1 \\ K_1(1) &= -\frac{3}{4} \\ L_0(0) &= -1 \\ L_1(0) &= -\frac{1}{4}. \end{aligned} \quad (\text{A.21})$$

These equations have been verified with the use of Gradshteyn and Ryzhik [16]

A.4 The Gamma Function

The gamma function, $\Gamma(w)$, is defined by the integral [17]

$$\Gamma(w) = a^w \int_0^\infty dz z^{w-1} e^{-az}, \quad \text{Re } w > 0 \quad (\text{A.22})$$

and satisfies some special relations

$$\Gamma(w+1) = w\Gamma(w) \quad (\text{A.23})$$

$$\Gamma(n+1) = n!, \quad n = 0, 1, 2, \dots \quad (\text{A.24})$$

$$\Gamma(1/2) = \sqrt{\pi}. \quad (\text{A.25})$$

The gamma function has poles at $0, -1, -2, \dots$. Near these poles, these gamma functions are expanded as follows,

$$\Gamma(-1 + \epsilon) = -\frac{1}{\epsilon} + \gamma - 1 + O(\epsilon) \quad (\text{A.26})$$

$$\Gamma(\epsilon) = \frac{1}{\epsilon} - \gamma + O(\epsilon) \quad (\text{A.27})$$

$$\Gamma(1 + \epsilon) = 1 - \gamma\epsilon + O(\epsilon) \quad (\text{A.28})$$

where γ is Euler's constant defined by

$$\gamma = \lim_{n \rightarrow \infty} \left[1 + \frac{1}{2} + \frac{1}{3} \dots + \frac{1}{n} - \ln n \right] = 0.577\ 215\ 664\ 9. \quad (\text{A.29})$$

Appendix B

Cavity modes

The cavity modes from the sources [7] and [18] are repeated here for convenience. These are used extensively in chapter 2. The eigenenergies, which have been numerically calculated, have been checked by calculating the gluon exchange between two quarks and verified with for example [18]-[22].

B.1 Quarks

The cavity modes of quarks are calculated in a static spherical cavity. The time independent Dirac equation is

$$(-i\vec{\gamma}\cdot\vec{\nabla} + m)u(p; \vec{r}) = \epsilon\gamma^0 u(p; \vec{r}), \quad (\text{B.1})$$

where the eigenmodes are given by

$$u(p; \vec{r}) = \begin{pmatrix} g_p(r)\chi_{\kappa\mu}(\hat{r}) \\ if_p(r)\chi_{-\kappa\mu}(\hat{r}) \end{pmatrix}. \quad (\text{B.2})$$

p summarizes the quantum labels as follows

$$p = \{\nu, \kappa, \mu\}, \quad (\text{B.3})$$

where ν, κ, μ stand for the radial, Dirac and magnetic quantum numbers respectively. The radial wave functions are given by

$$g_p(r) = N_p j_l(k_p r) \quad (\text{B.4})$$

$$f_p(r) = \frac{N_p \text{sgn}(\kappa) k_p}{(\epsilon_p + m)} j_l(k_p r). \quad (\text{B.5})$$

The total angular momenta, j , the orbital angular momenta, l and \bar{l} can be written in terms of κ as follows

$$j(\kappa) = \text{mod}(\kappa) - 1/2 \quad (\text{B.6})$$

$$l(\kappa) = j(\kappa) + \text{sgn}(\kappa)/2 \quad (\text{B.7})$$

$$\bar{l}(\kappa) = j(\kappa) - \text{sgn}(\kappa)/2. \quad (\text{B.8})$$

The boundary conditions used are

$$(i\vec{\gamma} \cdot \hat{r} + 1)u(\vec{r})|_{r=R} = 0. \quad (\text{B.9})$$

which can be simplified by using the solutions of the Dirac equation to

$$j_l(k_p) + \frac{k_p \text{sgn}(\kappa)}{(\epsilon_p + m)} j_{\bar{l}}(k_p) = 0. \quad (\text{B.10})$$

The normalization constant is given by

$$N_p^{-2} = R^3 [2\epsilon_p(\epsilon_p + \kappa) + m] \left[\frac{j_l(k_p)}{k_p} \right]^2. \quad (\text{B.11})$$

The energy of the cavity mode is given by

$$\epsilon_p = \text{sgn}(\nu) [k_p^2 + m^2]^{1/2}, \quad (\text{B.12})$$

if ν is allowed to label negative energy states. The eigenmodes satisfy the orthonormality and completeness relations, ie.,

$$\sum_{\alpha} \int d\vec{r} u_{\alpha}^{\dagger}(p; \vec{r}) u_{\alpha}(p'; \vec{r}) = \delta(p, p') \quad (\text{B.13})$$

$$\sum_p u_{\beta}(p; \vec{r}') u_{\alpha}^*(p; \vec{r}) = \delta(\vec{r}, \vec{r}') \delta_{\alpha\beta}, \quad (\text{B.14})$$

where $u_{\alpha}(p; \vec{r})$ denotes the α component of the Dirac spinor $u(p; \vec{r})$.

B.2 Gluons

The same treatment as used for the quarks is followed here. This time the starting point is the time independent d'Alembert equations, namely

$$(\nabla^2 + \Omega^2)a^{\mu} = 0. \quad (\text{B.15})$$

There are four polarizations which the eigenmodes come in, namely, the scalar, longitudinal, transverse magnetic and transverse electric which are

labeled as $\Sigma = 0, L, M, E$ respectively. The compact notation $p = \{N, J, M\}$, N, J, M being the radial, angular momentum and the magnetic quantum numbers respectively is also introduced. The expansion of a is as follows. For the scalar part

$$a^0(\Sigma = 0, p; \vec{r}) = N_{0p} i j_l(\Omega_{0p} r) Y_{JM}(\hat{r}) \quad (\text{B.16})$$

and for $\Sigma = L, M, E$

$$\vec{a}(\Sigma, p; \vec{r}) = N_{\Sigma p} \sum_{L=|J-1|}^{L=J+1} \alpha_{JL}^{\Sigma} j_L(\Omega_{\Sigma p} r) \vec{Y}_{JLM}(\hat{r}). \quad (\text{B.17})$$

The non-zero coefficients α_{JL}^{Σ} are given by

$$\begin{aligned} \alpha_{J,J-1}^L &= \sqrt{\frac{J}{2J+1}} & \alpha_{J,J+1}^L &= \sqrt{\frac{J+1}{2J+1}} \\ \alpha_{J,J}^M &= 1 & & \\ \alpha_{J,J-1}^E &= \sqrt{\frac{J+1}{2J+1}} & \alpha_{J,J+1}^E &= -\sqrt{\frac{J}{2J+1}}. \end{aligned} \quad (\text{B.18})$$

The M.I.T. bag model boundary conditions are

$$\begin{aligned} \hat{r} \cdot \vec{\nabla} a^0(\vec{r})|_{r=R} &= 0 \\ \hat{r} \cdot \vec{a}(\vec{r})|_{r=R} &= 0 \\ \hat{r} \times (\vec{\nabla} \times \vec{a}(\vec{r}))|_{r=R} &= 0. \end{aligned} \quad (\text{B.19})$$

These reduce to

$$\frac{d}{dr} j_J(\Omega_{0p} r)|_{r=R} = 0 \quad (\text{B.20})$$

$$\frac{d}{dr} j_J(\Omega_{Lp} r)|_{r=R} = 0 \quad (\text{B.21})$$

$$\frac{d}{dr} [r j_J(\Omega_{Mp} r)]|_{r=R} = 0 \quad (\text{B.22})$$

$$j_J(\Omega_{Ep} r)|_{r=R} = 0. \quad (\text{B.23})$$

Note that $\Omega_{0p} = \Omega_{Lp}$. The corresponding normalization constants are given by

$$N_{0p}^2 = N_{Lp}^2 = R^3 \frac{1}{2} j_J^2(\Omega_{0p}) \left[1 - \frac{J(J+1)}{\Omega_{0p}^2} \right] \quad (\text{B.24})$$

$$N_{Mp}^2 = R^3 \frac{1}{2} j_J^2(\Omega_{Mp}) \left[1 - \frac{J(J+1)}{\Omega_{Mp}^2} \right] \quad (\text{B.25})$$

$$N_{Ep}^2 = R^3 \frac{1}{2} j_{J+1}^2(\Omega_{Ep}). \quad (\text{B.26})$$

The metric tensor in polarization space is

$$g^{\Sigma\Sigma'} = \text{diag}\{1, -1, -1, -1\} \quad (\text{B.27})$$

which allows the orthonormality and completeness relations to be written as

$$\int d\vec{r} g^{\mu\nu} a_\mu^*(\Sigma', p; \vec{r}) a_\nu(\Sigma, p; \vec{r}) = g^{\Sigma\Sigma'} \delta(p, p') \quad (\text{B.28})$$

$$\sum_{\Sigma p} g^{\Sigma\Sigma} a^\mu(\Sigma, p; \vec{r}) a^{\nu*}(\Sigma, p; \vec{r}') = g^{\mu\nu} \delta(\vec{r}, \vec{r}'). \quad (\text{B.29})$$

Finally, $a^{\mu*}$ is related to a^μ by

$$a^{\mu*}(\Sigma, p; \vec{r}) = \eta_\Sigma (-1)^M a^\mu(\Sigma, p^*; \vec{r}) \quad (\text{B.30})$$

where $p^* = \{N, J, -M\}$ and the phase η_Σ stands for

$$\eta_\Sigma = \begin{cases} +1 & \Sigma = L, E \\ -1 & \Sigma = 0, M \end{cases} \quad (\text{B.31})$$

Appendix C

The Vertex Integrals

Here, the compact notation used for the vertex integrals is introduced and the sum rule test to check them is established.

C.1 The qqq Vertex

The vertex integrals are given by

$$Q_{p_1 p_2}^{\Sigma p_3} = i \int d\vec{r} \bar{u}(p_1; \vec{r}) \gamma_\mu u(p_2; \vec{r}) a^\mu(\Sigma, p_3; \vec{r}) \quad (\text{C.1})$$

$$\begin{aligned} \tilde{Q}_{p_1 p_2}^{\Sigma p_3} &= i \int d\vec{r} \bar{u}(p_1; \vec{r}) \gamma_\mu u(p_2; \vec{r}) a^{\mu*}(\Sigma, p_3; \vec{r}) \\ &= (-1)^M \eta_\Sigma Q_{p_1 p_2}^{\Sigma p_3*} = -Q_{p_1 p_2}^{\Sigma p_3}. \end{aligned} \quad (\text{C.2})$$

The angular and radial dependence are separated as follows:

$$\begin{aligned} Q_{p_1 p_2}^{\Sigma p_3} &= R_{p_1 p_2}^{\Sigma p_3} \int d\hat{r} \chi_{\kappa_1 \mu_1}^\dagger(\hat{r}) Y_{J_3 M_3}(\hat{r}) \chi_{\kappa_2 \mu_2}(\hat{r}) \quad \Sigma = 0, L, E \\ Q_{p_1 p_2}^{\Sigma p_3} &= R_{p_1 p_2}^{\Sigma p_3} \int d\hat{r} \chi_{\kappa_1 \mu_1}^\dagger(\hat{r}) Y_{J_3 M_3}(\hat{r}) \chi_{-\kappa_2 \mu_2}(\hat{r}) \quad \Sigma = M \end{aligned} \quad (\text{C.3})$$

The angular integral is given by [23]

$$\begin{aligned} \int d\hat{r} \chi_{\kappa \mu}^\dagger Y_{JM} \chi_{\kappa' \mu'} &= (-1)^{\mu+1/2} \sqrt{\frac{(2j+1)(2J+1)(2j'+1)}{4\pi}} \\ &\times \frac{(-1)^{l+J+l'} + 1}{2} \begin{pmatrix} j & J & j' \\ \frac{1}{2} & 0 & -\frac{1}{2} \end{pmatrix} \begin{pmatrix} j & J & j' \\ -\mu & M & \mu' \end{pmatrix} \end{aligned} \quad (\text{C.4})$$

and the radial integrals are given by

$$R_{p_1 p_2}^{Sp} = -N_{Sp} \int_0^R dr r^2 j_J(\Omega_{Sp} r) S_{p_1 p_2}(r) \quad (C.5)$$

$$R_{p_1 p_2}^{Lp} = \frac{\epsilon_{p_2} - \epsilon_{p_1}}{\Omega_{Lp}} R_{p_1 p_2}^{Sp} \quad (C.6)$$

$$R_{p_1 p_2}^{Mp} = \frac{\kappa + \kappa'}{\sqrt{J(J+1)}} N_{Mp} \int_0^R dr r^2 j_J(\Omega_{Mp} r) T_{p_1 p_2}(r) \quad (C.7)$$

$$R_{p_1 p_2}^{Ep} = \frac{N_{Ep}}{\Omega_{Ep} \sqrt{J(J+1)}} \int_0^R dr r^2 \{ J(J+1) j_J(\Omega_{Ep} r) U_{p_1 p_2}(r) \\ + (\kappa - \kappa') [J j_J(\Omega_{Ep} r) - \Omega_{Ep} r j_{J-1}(\Omega_{Ep} r)] T_{p_1 p_2}(r) \}, \quad (C.8)$$

where the radial functions

$$S_{p_1 p_2} = g_{p_1} g_{p_2} + f_{p_1} f_{p_2} \quad (C.9)$$

$$T_{p_1 p_2} = g_{p_1} f_{p_2} + f_{p_1} g_{p_2} \quad (C.10)$$

$$U_{p_1 p_2} = g_{p_1} f_{p_2} - f_{p_1} g_{p_2} \quad (C.11)$$

which are given in terms of the radial functions [18] have been introduced.

C.2 The qqq Sum Rule

In this section, the notation used by Stoddart [7] is introduced, as well as the same sum rule. The factor $M(p, p', p_1, p_2, \Sigma)$ is defined by

$$M(p, p', p_1, p_2, \Sigma) = \sum_{\mu_2 M_2} 4\pi g^{\Sigma\Sigma} Q_{pp_1}^{\Sigma p_2} \tilde{Q}_{p_1 p'}^{\Sigma p_2}, \quad (C.12)$$

where p and p' label the incoming and outgoing quark, p_1 labels the intermediate quark, and p_2 and Σ label the gluon. The result for $j = j'$,

$$M(p, p', p_1, p_2, \Sigma) = g^{\Sigma\Sigma} S_{pp_1}^{\Sigma p_2} S_{p_1 p'}^{\Sigma p_2} (2j_1 + 1)(2J_2 + 1) \times \\ \left(\begin{matrix} j_1 & J_2 & j' \\ \frac{1}{2} & 0 & -\frac{1}{2} \end{matrix} \right)^2 \delta_{j_m, j'_m} \quad (C.13)$$

where

$$S_{p_1 p_2}^{\Sigma p} = \frac{(-1)^{l+J+l'} + 1}{2} R_{p_1 p_2}^{\Sigma p}. \quad (C.14)$$

To test $M(p, p', p_1, p_2, \Sigma)$, the summation over p_1 is used. This yields

$$\sum_{p_1} M(p, p', p_1, p_2, \Sigma) = -4\pi \sum_{M_2} \int d\vec{r} \psi^\dagger(p; \vec{r}) \psi(p'; \vec{r}) A^\mu(\Sigma, p_2; \vec{r}) A_\mu^*(\Sigma, p_2; \vec{r}) \quad (\text{C.15})$$

$$= -(2J_2 + 1) \int dr r^2 \Phi(\Sigma, p_2; r) \times (g(p; r)g(p'; r) + f(p; r)f(p'; r)), \quad (\text{C.16})$$

where Φ is given by

$$\begin{aligned} \Phi(0, p) &= N_{0p}^2 j_J^2(\Omega_{0p} r) \\ \Phi(L, p) &= -N_{Lp}^2 \left[\frac{J+1}{2J+1} j_{J+1}^2(\Omega_{Lp} r) + \frac{J}{2J+1} j_{J-1}^2(\Omega_{Lp} r) \right] \\ \Phi(M, p) &= -N_{Mp}^2 j_J^2(\Omega_{Mp} r) \\ \Phi(E, p) &= -N_{Ep}^2 \left[\frac{J}{2J+1} j_{J+1}^2(\Omega_{Ep} r) + \frac{J+1}{2J+1} j_{J-1}^2(\Omega_{Ep} r) \right]. \end{aligned} \quad (\text{C.17})$$

The right hand side of eq.(C.15) can be computed directly thus a test of eq.(C.13) is obtained.

Bibliography

- [1] J. Baacke, Y. Igarashi, G. Kasperidus, H. Usler : Loop calculations in confined QCD : *Z.Phys.C* 21 (1983) 127
- [2] T.H. Hansson and R.L. Jaffe, The multiple reflection expansion for confined scalar, Dirac, and Gauge Fields, *Ann. of Phys.(N.Y.)* 151 (1983) 204
- [3] T.H. Hansson and R.L. Jaffe, Cavity Quantum Chromodynamics, *Phys. Rev. D* 28(1983) 882
- [4] S.N. Goldhaber, R.L. Jaffe, T.H. Hansson : The Self Energy of a confined quark : *Phys. Lett.* 131B (1983) 445
- [5] S.N. Goldhaber, The Self Energy of a confined quark, Ph.D. thesis, Massachusetts Institute of Technology, 1984
- [6] S.N. Goldhaber, R.L. Jaffe, T.H. Hansson : The Self Energy of a confined massive quark : *Nucl. Phys.* B277 (1986) 674
- [7] A.J. Stoddart : Renormalization of Cavity Field Theories , Ph.D thesis, University of Cape Town, UCT-TP 139/90
- [8] A.J. Stoddart and R. D. Viollier : Evaluating Loop Diagrams in a Cavity : (I) The Quark Self-Energy : *Nucl. Phys.* A532 (1991) 657
- [9] C.A. Dominguez and E. De Rafael : Light Quark Masses in QCD from Local Duality : *Ann. of Phys.* 174 (1987) 372
- [10] C.A. Dominguez, C. van Gend and N. Paver : QCD determination of the strange-quark mass : *Phys. Lett. B*, 253 (1991) 241
- [11] P. Pascual and R. Tarrach : QCD : Renormalization for the Practitioner, Springer-Verlag, Heidelberg, 1983

- [12] Ta-Pei Ching and Ling-Fong Li : Gauge theory of elementary particle physics - Oxford Science Publications.
- [13] C. Nash : Relativistic Quantum Fields : Academic Press 1978
- [14] Discussion with Gary Tupper on renormalization
- [15] A.B. Migdal : Qualitative Methods in Quantum Theory : W.A. Benjamin, Inc. 1977 pg140
- [16] Tables of Series, Integrals and Products, I.S.GradshTEYN, and I.M. Ryzhik, 4th Edition, 1965, Academic Press, London
- [17] Pocketbook of Mathematical Functions, M. Abramowitz, I.A. Stegun, Verlag Harri Deutsch - Thun; Frankfurt/Main 1984
- [18] R.F. Buser, R.D. Viollier, and P. Zimak : Canonical Quantization and Chromodynamics in a Spherical Cavity : International Journal Theor. Phys. 27 (1988) 925
- [19] T. DeGrand, R.L. Jaffe, K. Johnson and J. Kiskis : Masses and other parameters of light hadrons : Phys. Rev. D 12 (1975) 2060
- [20] K. Johnson : M.I.T. Bag Model : Acta Physica Polonica, B6 (1975) 865
- [21] S.A. Chin, A.K. Kerman, R.D. Viollier : On the spherical bag : Nucl. Phys. A407 (1983) 269
- [22] CERN 77-18 20 Oct 1977 : Proceedings of the 1977 CERN - JINR School of Physics
- [23] A. R. Edmonds, Angular Momentum in Quantum Mechanics, Princeton University Press, Princeton, New Jersey, 1957